0022-3565/10/3322-612–621$20.00
THE JOURNAL OF PHARMACOLOGY AND EXPERIMENTAL THERAPEUTICS
JPET 332:612–621, 2010

Vol. 332, No. 2
160275/3547959
Printed in U.S.A.

Lobelane Inhibits Methamphetamine-Evoked Dopamine Release via Inhibition of the Vesicular Monoamine Transporter-2[S]

Justin R. Nickell, Sairam Krishnamurthy, Seth Norrholm, Gabriela Deaciuc, Kiran B. Siripurapu, Guangrong Zheng, Peter A. Crooks, and Linda P. Dwoskin

Department of Pharmaceutical Sciences, College of Pharmacy, University of Kentucky, Lexington, Kentucky

Received August 10, 2009; accepted October 23, 2009

ABSTRACT

Lobeline is currently being evaluated in clinical trials as a methamphetamine abuse treatment. Lobeline interacts with nicotinic receptor subtypes, dopamine transporters (DATs), and vesicular monoamine transporters (VMAT2s). Methamphetamine inhibits VMAT2 and promotes dopamine (DA) release from synaptic vesicles, resulting ultimately in increased extracellular DA. The present study generated structure-activity relationships by defunctionalizing the lobeline molecule and determining effects on [^{3}H]dihydrotetrabenazine binding, inhibition of [^{3}H]DA uptake into striatal synaptic vesicles and synaptosomes, the mechanism of VMAT2 inhibition, and inhibition of methamphetamine-evoked DA release. Compared with lobeline, the analogs exhibited greater potency inhibiting DA transporter (DAT) function. Saturated analogs, lobelane and *nor*-lobelane, exhibited high potency (K_i = 45 nM) inhibiting vesicular [^{3}H]DA uptake, and lobelane competitively inhibited VMAT2 function. Lobeline and lobelane exhibited 67- and 35-fold greater potency, respectively, in inhibiting VMAT2 function compared to DAT function. Lobelane potently decreased (IC_{50} = 0.65 μM; I_{max} = 73%) methamphetamine-evoked DA overflow, and with a greater maximal effect compared with lobeline (IC_{50} = 0.42 μM, I_{max} = 56.1%). These results provide support for VMAT2 as a target for inhibition of methamphetamine effects. Both *trans*-isomers and demethylated analogs of lobelane had reduced or unaltered potency inhibiting VMAT2 function and lower maximal inhibition of methamphetamine-evoked DA release compared with lobelane. Thus, defunctionalization, *cis*-stereochemistry of the side chains, and presence of the piperidino *N*-methyl are structural features that afford greatest inhibition of methamphetamine-evoked DA release and enhancement of selectivity for VMAT2. The current results reveal that lobelane, a selective VMAT2 inhibitor, inhibits methamphetamine-evoked DA release and is a promising lead for the development of a pharmacotherapeutic for methamphetamine abuse.

Treatment center admissions involving methamphetamine abuse have more than doubled between 1995 and 2005 [Substance Abuse and Mental Health Services Administration, 2008], indicating the need for effective pharmacotherapies. There are currently no approved medications to treat methamphetamine abuse. Methamphetamine abuse liability stems from its reinforcing and rewarding effects demonstrated by use of animal models of intravenous methamphetamine self-administration and conditioned place preference, respectively (Yokel and Pickens, 1973; Hart et al., 2001, Xu et al., 2008). Brain dopaminergic pathways are activated by methamphetamine (Di Chiara and Imperato, 1988; Gold et al., 1989; Wise, 2002). Methamphetamine releases dopamine (DA) from synaptic vesicles into the cytosol via an interaction with the vesicular monoamine transporter (VMAT2) and by disruption of the vesicular proton gradient because of its weak basicity and high lipophilicity (Sulzer and Rayport, 1990; Pifl et al., 1995; Brown et al., 2000, 2001; Fleckenstein et al., 2007). Subsequently, available cytosolic DA is reverse-transported by the DA transporter (DAT) into the extracellular space (Sulzer et al., 1995). In addition, methamphetamine inhibits monoamine oxidase (MAO), preventing DA metabolism into dihydroxyphenylacetic acid (DOPAC) and increasing cytosolic DA (Mantle et al., 1976). VMAT2 is an

This work was supported by the National Institutes of Health [Grants DA13519, MH47611, DA16176].

The University of Kentucky holds patents on lobeline and the analogs described in the current work, which have been licensed by Yaupon Therapeutics, Inc. A potential royalty stream to L.P.D. and P.A.C. may occur consistent with University of Kentucky policy. Both L.P.D. and P.A.C. are founders of and have financial interest in Yaupon Therapeutics.

Article, publication date, and citation information can be found at http://jpet.aspetjournals.org.
doi:10.1124/jpet.109.160275.

[S] The online version of this article (available at http://jpet.aspetjournals.org) contains supplemental material.

ABBREVIATIONS: MAO, monoamine oxidase; ANOVA, analysis of variance; DA, dopamine; DAT, dopamine transporter; DOPAC, dihydroxyphenylacetic acid; DTBZ, dihydrotetrabenazine; METH, methamphetamine; MTD, *meso*-transdiene; *nor*-MTD, *nor-meso*-transdiene; *nor*-(±)-TTD, (±)-*nor-trans*-transdiene; nAChR, neuronal nicotinic acetylcholine receptor; Ro4-1284, (2*R*,3*S*,11b*S*)-2-ethyl-3-isobutyl-9,10-dimethoxy-2,2,4,6,7,11b-hexahydro-1*H*-pyrido[2,1-a]isoquinolin-2-ol; SAR, structure-activity relationship; (±)-TTD, (±)-*trans*-transdiene; (−)-TTD, (−)-*trans*-transdiene; (+)-TTD, (+)-*trans*-transdiene; VMAT2, vesicular monoamine transporter.

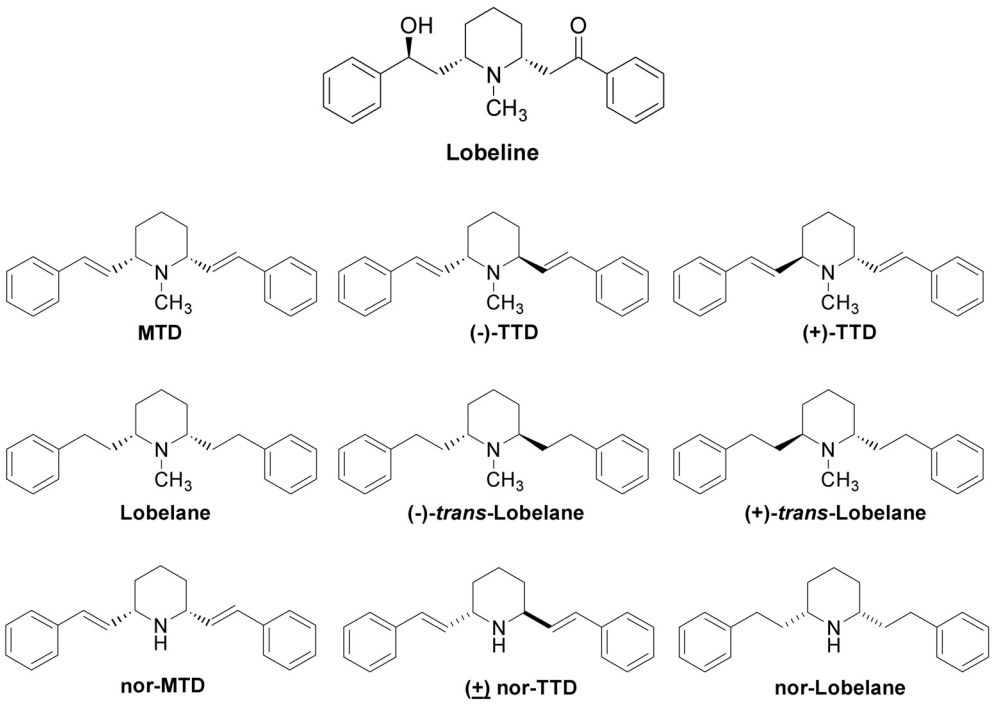

Fig. 1. Chemical structures of lobeline and its defunctionalized analogs. MTD is a defunctionalized, unsaturated *meso*-analog of lobeline. (−)-TTD and (+)-TTD are enantiomers and *trans*-isomers of MTD. Lobelane is a defunctionalized, saturated *meso*-analog of lobeline. (−)-*trans*-Lobelane and (+)-*trans*-lobelane are enantiomers and *trans*-isomers of lobelane. *nor*-MTD, *nor*-lobelane, and (±)-*nor*-TTD are demethylated analogs of MTD, lobelane, and (±)-TTD, respectively.

essential cellular component contributing to the increased extracellular DA concentrations and conditioned place preference (reward) induced by methamphetamine (Takahashi et al., 1997; Patel et al., 2003), which provides support for VMAT2 as a pharmacological target for the development of treatments for methamphetamine abuse.

Lobeline (Fig. 1), the major alkaloid of *Lobelia inflata*, attenuates methamphetamine self-administration in rats, but not by acting as a substitute reinforcer (Harrod et al., 2001, 2003), suggesting that it has potential as a low-abuse liability treatment for methamphetamine abuse. In addition, lobeline attenuates both methamphetamine-induced hyperactivity in locomotor activity assays and methamphetamine interoceptive cues in drug discrimination assays (Miller et al., 2001). Lobeline has been reported to act as a nicotinic receptor (nAChR) agonist (Decker et al., 1993) and as a nAChR antagonist (Teng et al., 1997, 1998; Briggs and McKenna, 1998; Toth and Vizi, 1998; Miller et al., 2000; Lim et al., 2004). Lobeline inhibits (IC_{50} = 80 μM) striatal [^{3}H]DA uptake via DAT, and more potently inhibits [^{3}H]dihydrotetrabenazine ([^{3}H]DTBZ) binding and [^{3}H]DA uptake via VMAT2 (IC_{50} = 0.90 and 0.88 μM, respectively; Teng et al., 1997, 1998). Lobeline inhibits (0.1–0.3 μM) *d*-amphetamine-evoked DA release from rat striatal slices (Miller et al., 2001) and methamphetamine-evoked DA release from VMAT2-transfected human embryonic kidney cells (Wilhelm et al., 2008). It is noteworthy that lobeline protects against methamphetamine neurotoxicity through its interaction at VMAT2 (Eyerman and Yamamoto, 2005). Thus, the mechanism by which lobeline decreases the behavioral effects of methamphetamine may be via interactions at nAChRs and/or neurotransmitter transporters.

With respect to nAChRs, initial generation of structure-activity relationships (SARs) revealed that both C2 and C6 piperidino ring substituents of lobeline are critical for interaction with α4β2* nAChRs (* indicates putative nAChR subtype assignment), as evaluated by inhibition of [^{3}H]cytisine binding to rat cortical membranes and stimulation of $^{86}Rb^+$ efflux from striatal synaptosomes (Terry et al., 1998). Lobeline fragments, containing either the phenylcarboxymethylene or phenylhydroxyethylene moiety, were less potent than lobeline at α4β2* nAChRs, indicating the importance of these moieties for optimal affinity at α4β2* (Flammia et al., 1999). Chemical defunctionalization (i.e., removal of the hydroxyl and keto functionalities) of the lobeline molecule was predicted to yield compounds with low affinity at nAChRs. As expected, lobelane and *meso*-transdiene (MTD; Fig. 1) had little or no affinity for either α4β2* or α7* nAChRs (Miller et al., 2004; Zheng et al., 2005). It is noteworthy that lobelane and MTD exhibited higher affinity for both DAT and VMAT2. In addition, changing the stereochemistry of the C2, C6 substituents in MTD from *cis* to *trans* afforded the isomeric analog, (−)-*trans*-transdiene [(−)-TTD; Fig 1], obtained as a pure optical isomer (Miller et al., 2004; Zheng et al., 2005). Likewise, (−)-TTD had little or no affinity for α4β2* and α7* nAChRs, and exhibited higher affinity at DAT than lobeline, and its affinity for VMAT2 was not different from lobeline (Miller et al., 2004). Thus, the oxygen functionalities and 2,6-*cis*-stereochemistry are important structural determinants for affinity of lobeline at α4β2* and α7* nAChRs, whereas defunctionalization increased affinity and selectivity for VMAT2.

The present study determined the affinity of lobeline and a wider range of defunctionalized lobeline analogs for VMAT2 and DAT, i.e., analog-induced inhibition of [^{3}H]DA uptake into isolated synaptic vesicles and synaptosomes, respectively. Mechanism of inhibition of VMAT2 function was determined for the best analog, lobelane, in the series. In addition, analogs were evaluated for inhibition of methamphetamine-evoked endogenous DA overflow from rat striatal slices. SAR trends emerging from these studies are of value in providing new leads in the development of clinical candidates for the treatment of methamphetamine abuse.

Materials and Methods

Animals. Male Sprague-Dawley rats (200–250 g upon arrival) were purchased from Harlan (Indianapolis, IN). Rats were housed in the Division of Laboratory Animal Resources at the College of Pharmacy at the University of Kentucky (Lexington, KY) and had ad libitum access to food and water. Experimental protocols involving the animals were in accordance with the *National Institutes of Health Guide for the Care and Use of Laboratory Animals* and were approved by the Institutional Animal Care and Use Committee at the University of Kentucky.

Materials. [^{3}H]DA (specific activity, 28.0 Ci/mmol) was purchased from PerkinElmer Life and Analytical Sciences (Boston, MA). [^{3}H]DTBZ (specific activity, 79.0 Ci/mmol) was a generous gift from Dr. Michael R. Kilbourn (Department of Internal Medicine and Neurology, University of Michigan, Ann Arbor, MI). Bovine serum albumin, EDTA, EGTA, L-(+)-tartaric acid, sucrose, magnesium sulfate, polyethyleneimine, adenosine 5′-triphosphate magnesium salt, HEPES, *S*(−)-nicotine ditartrate (nicotine), 3-hydroxytyramine (dopamine, DA), DOPAC, *d*-methamphetamine hydrochloride (methamphetamine), sodium chloride, magnesium sulfate and ascorbate oxidase were purchased from Sigma-Aldrich (St. Louis, MO). α-D-Glucose, L-ascorbic acid, and monobasic potassium phosphate were purchased from Aldrich Chemical Co. (Milwaukee, WI), AnalaR-BHD Ltd. (Poole, UK) and Mallinckrodt (St. Louis, MO), respectively. Perchloric acid (70%) was purchased from Mallinckrodt Baker (Phillipsburg, NJ). Ro4-1284 was obtained from Hoffman-La Roche Ltd. (Basel, Switzerland). Lobeline hemisulfate was purchased from ICN Biomedicals Inc. (Costa Mesa, CA). All other commercial chemicals were purchased from Fisher Scientific Co. (Pittsburgh, PA).

The lobeline analogs, MTD, (−)-TTD, (+)-*trans*-transdiene [(+)-TTD], lobelane, (−)-*trans*-lobelane, (+)-*trans*-lobelane, *nor*-MTD, (±)-*nor*-TTD, and *nor*-lobelane were synthesized according to reported methods (Zheng et al., 2005) and their structures are illustrated in Fig. 1. The structures of the lobeline analogs were verified by ^{1}H and ^{13}C NMR spectroscopy, mass spectrometry, and, in some instances, X-ray crystallography.

Synaptosomal [^{3}H]DA Uptake Assay. Inhibition of [^{3}H]DA uptake into rat striatal synaptosomes was conducted according to previously reported methods (Teng et al., 1997), with slight modification. Striata from individual rats were homogenized in ice-cold sucrose solution containing 5 mM $NaHCO_3$, pH 7.4, with 16 up-and-down strokes of a Teflon pestle homogenizer (clearance ≈ 0.003 inch). Homogenates and resulting supernatants were centrifuged at 2000*g* for 10 min at 4°C and 20,000*g* for 17 min, respectively. The pellet was then resuspended in 2.4 ml of assay buffer (125 mM NaCl, 5 mM KCl, 1.5 mM $MgSO_4$, 1.25 mM $CaCl_2$, 1.5 mM KH_2PO_4, 10 mM D-glucose, 25 mM HEPES, 0.1 mM EDTA, 0.1 mM pargyline, 0.1 mM ascorbic acid, saturated with 95% 0_2/5% CO_2, pH 7.4). The assay was performed in duplicate in a total volume of 500 μl. Aliquots of the vesicular suspension (25 μl) were added to tubes containing assay buffer and various concentrations of analog (100 μM to 1 nM), and incubated at 34°C for 5 min. Nonspecific uptake was determined in the presence of nomifensine (10 μM). Samples were placed on ice, and 50 μl of 0.1 μM [^{3}H]DA was added to each tube, after which accumulation was permitted to proceed for 10 min at 34°C. The reaction was terminated by the addition of 3 ml of ice-cold assay buffer and subsequent filtration. Radioactivity retained by the GF/B filters (presoaked for 2 h in assay buffer) was determined by liquid β-scintillation spectrometry.

[^{3}H]DTBZ Binding Assay. Lobeline- and analog-induced inhibition of [^{3}H]DTBZ binding was determined by use of modifications of a method described previously (Teng et al., 1998). Rat whole brain (excluding cerebellum) or striatum was homogenized in 20 ml of ice-cold 0.32 M sucrose solution with seven up-and-down strokes of a Teflon pestle homogenizer (clearance ≈ 0.003 inch). Homogenates were centrifuged at 1000*g* for 12 min at 4°C, and the resulting supernatants were again centrifuged at 22,000*g* for 10 min at 4°C. Resulting pellets were incubated in 18 ml of ice-cold water for 5 min, and 2 ml of HEPES (25 mM) and potassium tartrate (100 mM) solution were subsequently added. Samples were centrifuged (20,000*g* for 20 min at 4°C), and 20 μl of $MgSO_4$ (1 mM) solution was then added to the supernatants. Solutions were centrifuged (100,000*g* for 45 min at 4°C) and pellets resuspended in ice-cold assay buffer (25 mM HEPES, 100 mM potassium tartrate, 5 mM $MgSO_4$, 0.1 mM EDTA, and 0.05 mM EGTA, pH 7.5). Assays were performed in duplicate by use of 96-well plates. Aliquots of vesicular suspension (15 μg of protein in 100 μl) were added to wells containing 5 nM [^{3}H]DTBZ, 50 μl of analog (1 nM to 1 mM), and 50 μl of buffer. Nonspecific binding was determined in the presence of Ro4-1284 (20 μM). Reactions were terminated by filtration (Packard Filtermate harvester; PerkinElmer Life and Analytical Sciences) onto Unifilter-96 GF/B filter plates (presoaked in 0.5% polyethyleneimine). Filters were subsequently washed five times with 350 μl of ice-cold buffer (25 mM HEPES, 100 mM potassium tartrate, 5 mM $MgSO_4$, and 10 mM NaCl, pH 7.5). Filter plates were dried and bottom-sealed, and each well was filled with 40 μl of scintillation cocktail (MicroScint 20; PerkinElmer Life and Analytical Sciences). Radioactivity on the filters was determined by liquid β-scintillation spectrometry (TopCount NXT; PerkinElmer Life and Analytical Sciences).

Vesicular [^{3}H]DA Uptake Assay. Inhibition of [^{3}H]DA uptake was conducted by use of a preparation of isolated synaptic vesicles as described previously (Teng et al., 1997). In brief, rat striata were homogenized with 10 up-and-down strokes of a Teflon pestle homogenizer (clearance ~ 0.003 inch) in 14 ml of 0.32 M sucrose solution. Homogenates were centrifuged (2000*g* for 10 min at 4°C), and the resulting supernatants were centrifuged again (10,000*g* for 30 min at 4°C). Pellets were resuspended in 2 ml of 0.32 M sucrose solution and subjected to osmotic shock by adding 7 ml of ice-cold water to the preparation, followed by the immediate restoration of osmolarity by adding 900 μl of 0.25 M HEPES buffer and 900 μl of 1.0 M potassium tartrate solution. Samples were centrifuged (20,000*g* for 20 min at 4°C), and the resulting supernatants were centrifuged again (55,000*g* for 1 h at 4°C), followed by the addition of 100 μl of 10 mM $MgSO_4$, 100 μl of 0.25 M HEPES, and 100 μl of 1.0 M potassium tartrate solution before the final centrifugation (100,000*g* for 45 min at 4°C). Final pellets were resuspended in 2.4 ml of assay buffer (25 mM HEPES, 100 mM potassium tartrate, 50 μM EGTA, 100 μM EDTA, 1.7 mM ascorbic acid, 2 mM ATP-Mg^{2+}, pH 7.4). Aliquots of the vesicular suspension (100 μl) were added to tubes containing assay buffer, various concentrations of analog (0.1 nM to 10 mM) and 0.1 μM [^{3}H]DA to produce a final volume of 500 μl. Nonspecific uptake was determined in the presence of Ro4-1284 (10 μM). Reactions were terminated by filtration, and radioactivity retained by the filters was determined as described previously.

To determine the mechanism of inhibition of [^{3}H]DA uptake for lobeline and lobelane, kinetic analyses were performed. Concentrations of lobeline (0.25 μM) and lobelane (0.024 μM) were chosen based on 0.5 × the K_i values obtained in the [^{3}H]DA uptake inhibition assays. Experiments were conducted in the absence (control) and presence of analog. Incubations were initiated by the addition of 50 μl of the vesicular suspension to 150 μl of assay buffer, 25 μl of analog, and 25 μl of a range of concentrations of [^{3}H]DA (0.001–5.0 μM). Nonspecific uptake was determined in the presence of Ro4-1284 (10 μM). After an incubation period of 8 min, [^{3}H]DA uptake was terminated by filtration, and radioactivity retained by the filters was determined as described previously.

Endogenous DA and DOPAC Overflow Assay. Coronal striatal slices were prepared and superfused as described previously (Teng et al., 1997). Slices were incubated in Krebs buffer (118 mM NaCl, 4.7 mM KCl, 1.2 mM $MgCl_2$, 1.0 mM NaH_2PO_4, 1.3 mM $CaCl_2$, 11.1 mM α-D-glucose, 25 mM $NaHCO_3$, 0.11 mM L-ascorbic acid, and 0.004 mM EDTA, pH 7.4, saturated with 95% O_2/5% CO_2) at 34°C for 60 min in a metabolic shaker. Each slice was then transferred to a

glass superfusion chamber and superfused at 1 ml/min for 60 min. Three 5-min samples (1 ml collected into 100 μl of 0.1 M perchloric acid) determined basal outflow of DA or DOPAC. Slices were superfused for 30 min in the absence or presence of a single concentration of analog (0.1 nM to 3 μM). Subsequently, methamphetamine (5 μM) was added to the superfusion buffer and slices were superfused for 15 min, followed by superfusion for another 20 min with analog in the absence of methamphetamine. Methamphetamine concentration and exposure time were chosen based on previously reported concentration-response curves (Liang and Rutledge, 1982; Bowyer et al., 1991), and concentrations of lobeline (0.1–3.0 μM) were chosen that did not deplete striatal DA content (Teng et al., 1997) and inhibited amphetamine-evoked DA overflow (Miller et al., 2000). In each experiment, a striatal slice was superfused for 80 min in the absence of analog or methamphetamine, and served as the buffer control condition. Duplicate slices were superfused with methamphetamine in the absence of analog, and served as the methamphetamine control condition.

Ascorbate oxidase (20 μl) was added to each superfusate sample (500 μl) and 100 μl of the resulting solution was injected onto the high-performance liquid chromatography-electrochemical detection unit, which consisted of a model 116 pump, model 508 autosampler (Beckman Coulter, Inc., Fullerton, CA), an ODS ultrasphere C18 reverse-phase 80 × 4.6 mm, 3-μm column, and a coulometric-II detector with model 5020 guard cell (+0.60 V) and model 5011 cell (E1 = −0.05 V, E2 = +0.32 V) (ESA, Inc., Chelmsford, MA). The eluent was 0.07 M citrate/0.1 M acetate buffer (pH 4) containing: 175 mg/liter octylsulfonic acid-sodium salt, 650 mg/liter NaCl, and 7% methanol. Separations were performed at room temperature at a flow rate of 1.5 ml/min, and required 5 to 6 min per sample. Retention times of DA and DOPAC standards were used to identify peaks. Peak heights were used to calculate the detected amounts of analyte based on standard curves. Detection limits for DA and DOPAC were 1 and 2 pg/100 μl, respectively.

To determine whether the high concentration of analog altered tissue DA content, slices were homogenized by sonication in 500 μl of perchloric acid immediately after perfusion of striatal slices with 3 μM each analog. In each experiment, two slices were perfused in the absence of analog and served as the control condition. The homogenate was centrifuged at 30,000*g* at 4°C for 15 min, and the supernatant was separated and filtered (0.22 μm). Filtrate (100 μl) was processed via high-performance liquid chromatography-electrochemical detection as described previously.

Data Analyses. For inhibition of [^{3}H]DTBZ binding, specific binding was determined by subtracting nonspecific binding from total binding. For inhibition of [^{3}H]DA uptake, specific uptake was determined by subtracting nonspecific uptake from total uptake. Concentrations of inhibitor that produced 50% inhibition of binding or uptake (IC_{50} values) were determined from the concentration-effect curves via an iterative curve-fitting program (Prism 4.0; GraphPad Software Inc., San Diego, CA). Inhibition constants (K_i values) were determined by use of the Cheng-Prusoff equation. For analysis of [^{3}H]DA uptake kinetics, K_m and V_{max} values were determined from concentration-effect curves for specific [^{3}H]DA uptake. Paired two-tailed *t* tests were performed on the log K_m and arithmetic V_{max} values to determine differences in the parameters between analog and control.

For the DA overflow assay, fractional release was defined as the concentration of DA and DOPAC in each 1-ml superfusate sample. Basal outflow was calculated from the average fractional release during the 15-min period before addition of analog to the superfusion buffer. Total DA or DOPAC overflow was calculated as the sum of the increases in fractional release above basal outflow during superfusion with methamphetamine or analog. Intrinsic activity of the analogs was the total overflow above basal outflow determined during the initial 30-min period of superfusion with the analog in the absence of methamphetamine. These data were analyzed by one-way repeated-measures ANOVA, and when appropriate followed by Dunnett's *t* test to determine differences between analog-evoked overflow and overflow in the control condition.

Total tissue DA content was determined immediately after the 30-min period of perfusion with each analog (3 μM). These data were also analyzed by one-way repeated-measures ANOVA, and when appropriate followed by Dunnett's *t* test to determine differences between DA content after application of analog and the control condition.

Lobeline- or analog-induced inhibition of methamphetamine-evoked DA or DOPAC overflow was determined during the 35-min period after exposure to methamphetamine, and was analyzed by one-way repeated-measures ANOVA. When appropriate, Dunnett's *t* tests were performed to determine differences between lobeline or analog and the methamphetamine control (absence of lobeline or analog). Analog concentrations that produced 50% inhibition (IC_{50} values) and maximal inhibition (I_{max}) were determined from the concentration-effect curves. One-way ANOVA followed by Tukey's test was performed to compare the I_{max} and IC_{50} values of lobeline and its analogs.

The time course for lobeline or analog-induced inhibition of methamphetamine-evoked fractional DA release was analyzed by use of two-way ANOVA with concentration and time as repeated-measures factors. Subsequently, a separate two-way ANOVA with concentration and time as repeated-measures factors was performed to compare the effect of methamphetamine (5 μM) with the buffer control. A separate two-way ANOVA was performed to compare lobeline or analog with the methamphetamine control. If the two-way ANOVA revealed a significant concentration × time interaction, then one-way repeated-measures ANOVAs were performed to determine the specific time points at which a concentration-dependent effect occurred, and Dunnett's *t* tests were performed as appropriate to determine the lobeline or analog concentrations that were significantly different from the methamphetamine control. IC_{50} values were determined by use of an iterative curve-fitting program (Prism 4.0; GraphPad Software Inc.). ANOVAs and post hoc tests were conducted with use of SPSS version 9.0 (SPSS Science, Chicago, IL). Statistical significance was defined as $p < 0.05$.

Results

Inhibition of [^{3}H]DA Uptake into Rat Striatal Synaptosomal Preparations. Lobeline- and analog-mediated inhibition of [^{3}H]DA uptake in synaptosomal preparations assessed inhibition of DAT function (Fig. 2). With the exception of lobeline (I_{max} = 80.7%), all compounds inhibited [^{3}H]DA uptake at DAT with a maximal inhibition >95%. Lobelane was 20-fold more potent in the inhibition of DAT than lobeline (K_i = 1.57 and 31.6 μM, respectively; $p < 0.05$). MTD exhibited 40-fold greater potency (K_i = 0.039 μM; $p < 0.05$) than lobelane and was equipotent with (−)-TTD (K_i = 0.22 μM), which had greater potency (K_i = 1.89 μM; $p < 0.05$) than (+)-TTD. The (−)- and (+)-*trans*-lobelane enantiomers possessed similar potency (K_i = 1.12 and 4.12 μM, respectively) in inhibition of DAT function, and were not different from lobelane. *N*-Demethylation of MTD and (−)-TTD resulted in a 5- to 16-fold reduction in potency ($p < 0.05$), whereas *N*-demethylation of lobelane resulted in a 5-fold increase in potency ($p < 0.05$). Methamphetamine inhibited (K_i = 0.11 μM) [^{3}H]DA uptake in the synaptosomal preparation.

Inhibition of [^{3}H]DTBZ Binding. [^{3}H]DTBZ binding assays were conducted using rat whole brain to maximize protein yield. However, vesicular [^{3}H]DA uptake assays that assess VMAT2 function were performed with use of striatal preparations. Because two different tissue preparations were

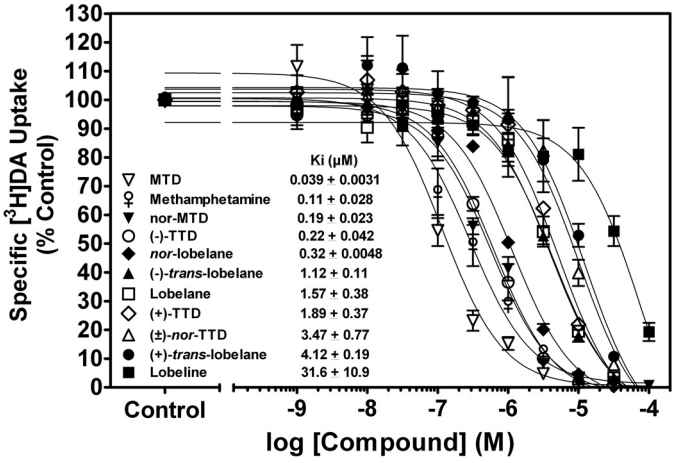

Fig. 2. Lobeline and its analogs inhibit specific [^{3}H]DA uptake into rat striatal synaptosomes. K_i values are presented in the legend in order of decreasing potency. Control represents [^{3}H]DA uptake in the absence of compound. Data are mean (± S.E.M.) specific [^{3}H]DA uptake as a percentage of the respective control (15.0 ± 1.65 pmol/min/mg, control n = 44 rats; n = 3–4 rats/compound).

used, the ability of two standard compounds, TBZ and Ro4-1284, to inhibit [^{3}H]DTBZ binding in these preparations was compared (Fig. 3). K_i values for both TBZ and Ro4-1284 were not different between whole brain and striatum. Thus, whole

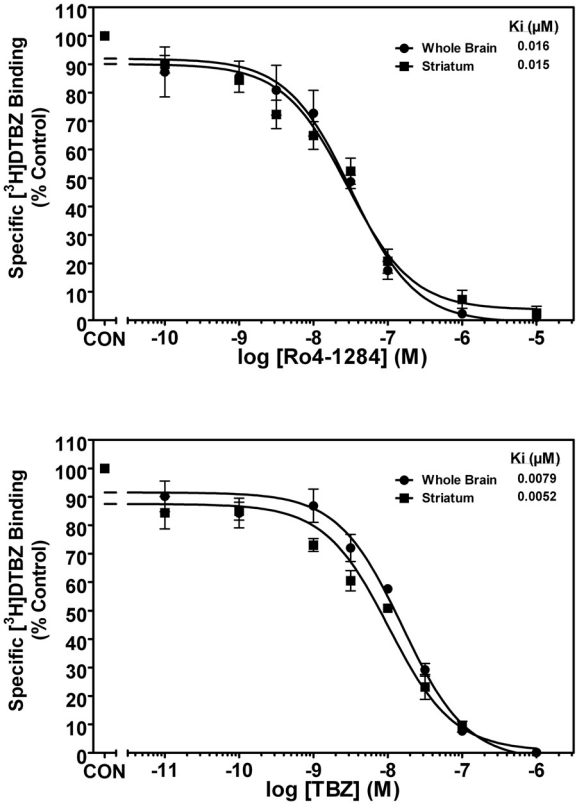

Fig. 3. Ro4-1284 and TBZ inhibition of [^{3}H]DTBZ binding assays conducted in rat whole brain versus striatal preparations. The affinity of two standards (Ro4-1284, top; TBZ, bottom) for the [^{3}H]DTBZ binding site located on VMAT2 were analyzed in both rat whole brain and striatal preparations. Control indicates the absence of the standard. Data indicate mean ± S.E.M. and are presented as a percentage of their respective controls (whole brain, 1225 ± 81.1 fmol/mg; striatum, 448.8 ± 20.2 fmol/mg; n = 3 rats/standard, per preparation).

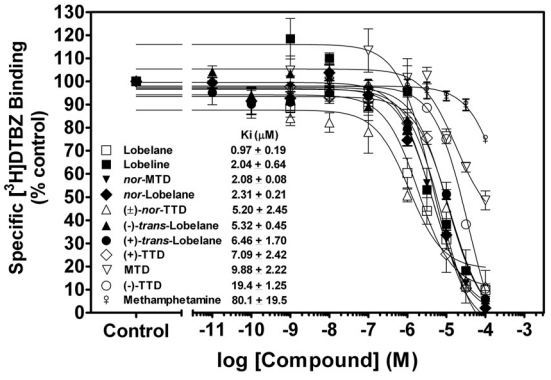

Fig. 4. Lobeline and its analogs inhibit specific [^{3}H]DTBZ binding to vesicle membranes prepared from rat whole brain. K_i values for lobeline and analogs are presented in the legend in order of decreasing affinity. Control represents specific [^{3}H]DTBZ binding in the absence of compound. Data are mean (± S.E.M.) specific [^{3}H]DTBZ binding presented as a percentage of the respective control (880 ± 153 fmol/mg, control n = 37 rats; n = 3–4 rats/compound).

brain and striatal preparations provide comparable data in the [^{3}H]DTBZ binding assay.

Lobeline and its analogs inhibited [^{3}H]DTBZ binding to synaptic vesicle membranes obtained from rat whole brain (Fig. 4). With the exception of MTD (I_{max} = 51.4%) and methamphetamine (I_{max} = 25.1%), all compounds exhibited a maximal inhibition of >85%. Lobeline inhibited (K_i = 2.04 μM) [^{3}H]DTBZ binding to VMAT2, and MTD had a lower affinity (K_i = 9.88 μM) in comparison ($p < 0.05$). Lobelane had 2-fold greater affinity (K_i = 0.97 μM; $p < 0.05$) than lobeline at VMAT2. (+)- and (−)-*trans*-Lobelane enantiomers possessed equivalent affinities (K_i = 6.46 and 5.32 μM, respectively), and had 5- to 6-fold lower affinity ($p < 0.05$) than lobelane. The 2,6-*trans*-analogs of MTD, (+)-TTD and (−)-TTD, had K_i values of 7.09 and 19.4 μM, respectively. *nor*-MTD and (±)-*nor*-TTD had K_i values of 2.08 and 5.20 μM, respectively. *N*-Demethylation of MTD and (−)-TTD enhanced affinity ($p < 0.05$) for VMAT2 by 5- and 4-fold, respectively. Methamphetamine had a low affinity (K_i = 80.1 μM) for the [^{3}H]DTBZ binding site.

Inhibition of [^{3}H]DA Uptake into Rat Striatal Synaptic Vesicles. Inhibition of [^{3}H]DA uptake into synaptic vesicle preparations by lobeline and its analogs is shown in Fig. 5. All

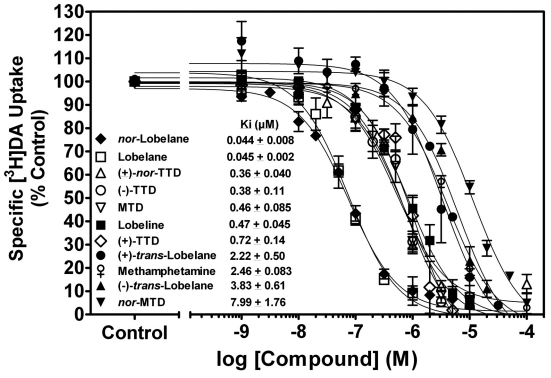

Fig. 5. Lobeline and its analogs inhibit specific [^{3}H]DA uptake into rat striatal synaptic vesicle preparations. K_i values are presented in the legend in order of decreasing potency. Control represents [^{3}H]DA uptake in the absence of compound. Data are mean (± S.E.M.) specific [^{3}H]DA uptake as a percentage of the respective control (40.5 ± 0.5 pmol/min/mg, control n = 46 rats; n = 4–5 rats/compound).

TABLE 1
DA content in striatal slices exposed to lobeline and its analogs

Compound (3 μM)	Total Tissue DA Content
	ng/mg
Control	16.4 ± 1.20
Lobeline	19.7 ± 5.50
MTD	23.3 ± 1.50
(−)-TTD	17.7 ± 1.90
(+)-TTD	15.2 ± 2.40
Lobelane	15.0 ± 2.17
(+)-*trans*-Lobelane	13.9 ± 1.58
nor-MTD	21.7 ± 5.00
(±)-*nor*-TTD	22.2 ± 3.90
nor-lobelane	20.2 ± 2.43

Data are mean ± S.E.M.; $n = 3$ experiments/compound.

compounds exhibited a maximal inhibition of [^{3}H]DA uptake of >90%. Lobeline inhibited [^{3}H]DA uptake with a K_i value of 0.47 μM, whereas lobelane and *nor*-lobelane exhibited a 10-fold increase in potency (K_i = 0.045 and 0.044 μM, respectively; $p < 0.05$) compared with lobeline. (+)- and (−)-*trans*-Lobelane exhibited a 5- and 9-fold reduction in potency (K_i = 2.22 and 3.83 μM, respectively; $p < 0.05$) compared with lobelane, and were equipotent with methamphetamine (K_i = 2.46 μM). MTD, (−)-TTD, and (+)-TTD all exhibited potencies (K_i = 0.46, 0.38, and 0.72 μM, respectively) not different from each other and not different from lobeline. (+)-*nor*-TTD exhibited a potency (K_i = 0.36 μM) similar to lobeline. In contrast, *nor*-MTD had the lowest potency (K_i = 7.99 μM) for inhibiting [^{3}H]DA uptake into synaptic vesicles.

To elucidate the mechanism of lobeline and lobelane interaction with VMAT2, kinetic analyses of [^{3}H]DA uptake into synaptic vesicles were conducted. Compared with control (K_m = 0.11 ± 0.0081 μM; V_{max} = 46.7 ± 7.92 pmol/min/mg) both lobeline (K_m = 0.29 ± 0.064 μM; V_{max} = 50.2 ± 7.80 pmol/min/mg) and lobelane (K_m = 0.38 + 0.051 μM; V_{max} = 57.1 ± 12.1 pmol/min/mg) significantly ($p < 0.05$) increased the K_m without altering V_{max}, indicating that these compounds inhibit [^{3}H]DA uptake in a competitive manner.

DA and DOPAC Overflow from Superfused Rat Striatal Slices. The ability of lobeline and its analogs (0.1–3.0 μM) to evoke DA and DOPAC overflow was assessed during the 30-min period of superfusion before the addition of methamphetamine (5 μM) to the superfusion buffer. At the highest concentration evaluated, lobeline and its analogs did not deplete striatal DA content (Table 1). In addition, these compounds alone did not evoke DA overflow (Table 2). In contrast, each compound alone increased DOPAC overflow (Fig. 6), with the exception of (±)-*nor*-TTD. Analysis of the effect of lobeline on DOPAC overflow revealed a concentration-dependent effect ($F_{4,16}$ = 4.14, $p < 0.05$). Post hoc analysis indicated that 3 μM lobeline increased DOPAC overflow (Fig. 6, top). Analysis of DOPAC overflow also revealed a concentration effect for MTD ($F_{4,13}$ = 19.94, $p < 0.001$), (−)-TTD ($F_{4,14}$ = 147.61, $p < 0.001$), and (+)-TTD ($F_{4,20}$ = 8.59, $p < 0.001$). The lowest concentration of MTD

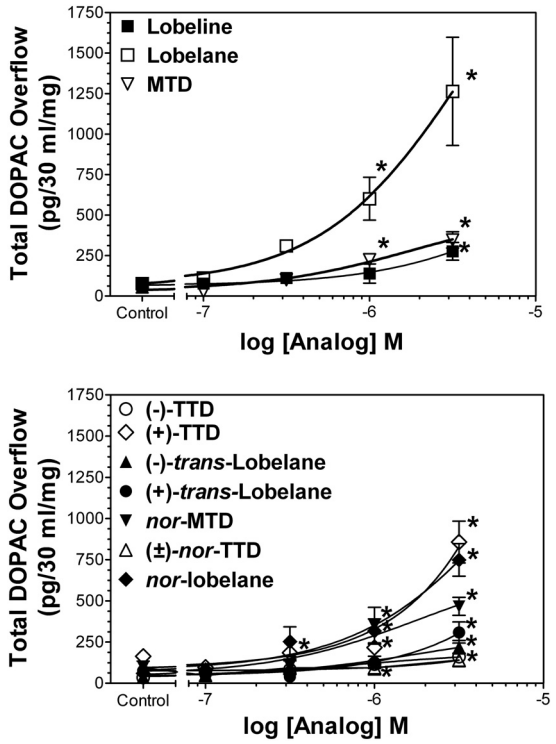

Fig. 6. Effect of lobeline, MTD, and their analogs on DOPAC overflow from rat striatal slices. Striatal slices were superfused with a range of concentrations of lobeline, lobelane, or MTD (top), and (−)-*trans*-lobelane, (+)-*trans*-lobelane, *nor*-MTD, (±)-*nor*-TTD, *nor*-lobelane, (−)-TTD or (+)-TTD (bottom). Data (pg/30 ml/mg) are expressed as mean ± S.E.M. and represent the 30-min period of superfusion in the absence or presence of lobeline or analog before the addition of methamphetamine to the buffer. Buffer control represents overflow from slices superfused in the absence of lobeline or analog (*, $p < 0.05$ different from buffer control; n = 4–7 rats/compound).

TABLE 2
Lobeline and its analogs do not increase DA overflow from rat striatal slices
Striatal slices were superfused with a range of concentrations of lobeline or analog. Data represent the 30-min period of superfusion in the absence or presence of lobeline or analogs.

	n	Concentration				
		0 [a]	0.1	0.3	1	3
				μM		
Lobeline	5	4.5 ± 2.0 [b]	1.0 ± 1.0	1.0 ± 1.0	5.0 ± 2.5	8.0 ± 5.5
MTD	5	7.0 ± 3.5	2.5 ± 1.5	7.0 ± 2.5	9.0 ± 3.5	9.0 ± 3.0
(−)-TTD	7	3.5 ± 2.5	3.5 ± 2.0	6.5 ± 2.0	3.5 ± 0.5	6.5 ± 2.5
(+)-TTD	5	3.5 ± 2.0	13 ± 8.5	22 ± 10	14 ± 7.0	18 ± 9.5
Lobelane	4	2.5 ± 1.5	0.0 ± 0.0	0.0 ± 0.0	9.5 ± 5.5	2.5 ± 1.5
(−))-*trans*-Lobelane	5	1.0 ± 0.5	2.0 ± 0.5	2.5 ± 1.5	3.0 ± 2.0	3.5 ± 3.5
(+)-*trans*-Lobelane	6	2.0 ± 1.5	3.5 ± 2.5	8.0 ± 3.5	5.5 ± 3.0	3.0 ± 1.5
nor-MTD	6	0.0 ± 0.0	0.0 ± 0.0	1.0 ± 1.0	1.0 ± 1.0	2.5 ± 2.5
(±)-*nor*-TTD	4	0.0 ± 0.0	0.0 ± 0.0	0.0 ± 0.0	0.0 ± 0.0	0.0 ± 0.0
nor-Lobelane	6	0.0 ± 0.0	1.5 ± 1.5	2.5 ± 2.5	0.0 ± 0.0	1.5 ± 1.5

[a] 0 indicates buffer control condition (superfusion with buffer only, in the absence of lobeline or analog).
[b] Data are expressed as pg/30 ml/mg (mean ± S.E.M.). n indicates number of rats/compound.

and (−)-TTD to increase ($p < 0.05$) DOPAC overflow was 1 μM, and the lowest concentration of (+)-TTD was 0.3 μM (Fig. 6, bottom). A concentration effect ($p < 0.001$) was found for lobelane ($F_{4,11} = 9.89$; Fig. 6, top), (−)-*trans*-lobelane ($F_{4,11} = 14.21$) and (+)-*trans*-lobelane ($F_{4,19} = 15.71$) to increase DOPAC overflow (Fig. 6, bottom). The lowest concentration of lobelane to increase ($p < 0.05$) DOPAC overflow was 1.0 μM, and for both (−)-*trans*-lobelane and (+)-*trans*-lobelane, the lowest concentration was 3.0 μM. A concentration effect ($p < 0.001$) for *nor*-MTD ($F_{4,18} = 13.1$) and *nor*-lobelane ($F_{4,18} = 26.93$) was found, whereas (±)-*nor*-TTD ($F_{4,11} = 1.797$, $p = 0.194$) did not increase DOPAC overflow (Fig. 6, bottom). The lowest concentration of both *nor*-MTD and *nor*-lobelane to increase ($p < 0.05$) DOPAC overflow was 1 μM.

Lobeline, MTD, and Lobelane Inhibition of Methamphetamine-Evoked DA Overflow. Lobeline-mediated inhibition of methamphetamine (5 μM)-evoked DA overflow and fractional DA release is illustrated in Fig. 7. Lobeline (0.3–3 μM) inhibited methamphetamine-evoked DA overflow ($IC_{50} = 0.42 \pm 0.10$ μM, $I_{max} = 56.1 \pm 4.18\%$), and a concentration effect ($F_{5,19} = 41.24$, $p < 0.001$) was found. The time course for lobeline to inhibit methamphetamine-evoked fractional DA release is shown in Fig. 8 (top). A significant concentration × time interaction ($F_{9,180} = 22.07$, $p < 0.01$) was found. Compared with the buffer control, methamphetamine evoked an increase in fractional DA release from 20 to 45 min after its addition to the superfusion buffer. A separate two-way repeated-measures ANOVA on the time course data revealed a concentration × time interaction ($F_{36,180} = 3.46$, $p < 0.01$). Lobeline (1.0–3.0 μM) decreased ($p < 0.05$) methamphetamine-evoked fractional DA release from 30 to 35 min.

Figure 7 also illustrates the concentration effect of MTD ($F_{5,19} = 49.62$, $p < 0.001$) on methamphetamine-evoked DA overflow. The lowest MTD concentration to produce inhibition was 0.1 μM ($IC_{50} = 0.44$ μM; $I_{max} = 76\%$). The time course for MTD inhibition of methamphetamine-evoked fractional DA release is illustrated in Fig. 8 (middle). Methamphetamine evoked a significant increase in fractional DA release from 15 to 30 min. Analysis of the time course for MTD to inhibit methamphetamine-evoked fractional DA release revealed a concentration × time interaction ($F_{36,180} = 6.75$, $p < 0.001$). MTD (1.0–3.0 μM) decreased ($p < 0.05$) methamphetamine-evoked fractional DA release from 25 to 35 min.

Figure 7 also illustrates the concentration-dependent inhibition of methamphetamine-evoked DA overflow by lobelane ($F_{5,14} = 11.91$, $p < 0.001$). The lowest lobelane concentration to inhibit methamphetamine-evoked DA overflow was 1 μM.

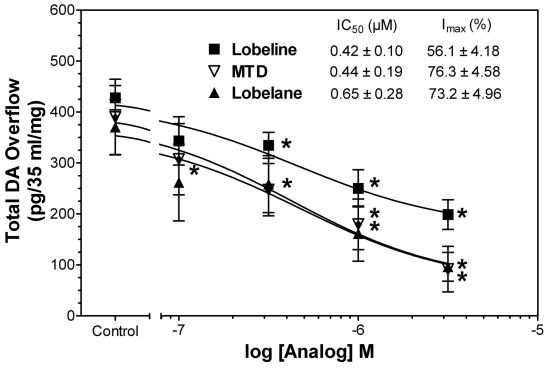

Fig. 7. Lobeline, MTD, and lobelane inhibition of methamphetamine-evoked DA overflow from rat striatal slices. Striatal slices were superfused with buffer for 60 min, and then superfusion continued for 30 min in the absence and presence of various concentrations of compound. Subsequently, slices were superfused for 15 min with buffer in which methamphetamine (5 μM) was added. Superfusion continued for an additional 20 min with compound in absence of methamphetamine. Thus, in each experiment, one striatal slice was superfused with buffer only, and two striatal slices were superfused with methamphetamine in the absence of compound, serving as buffer and methamphetamine controls, respectively. Data are expressed as pg/35 ml/mg (mean ± S.E.M) (*, $p < 0.05$ different from methamphetamine control at the respective time point; $n = 5$ rats/compound).

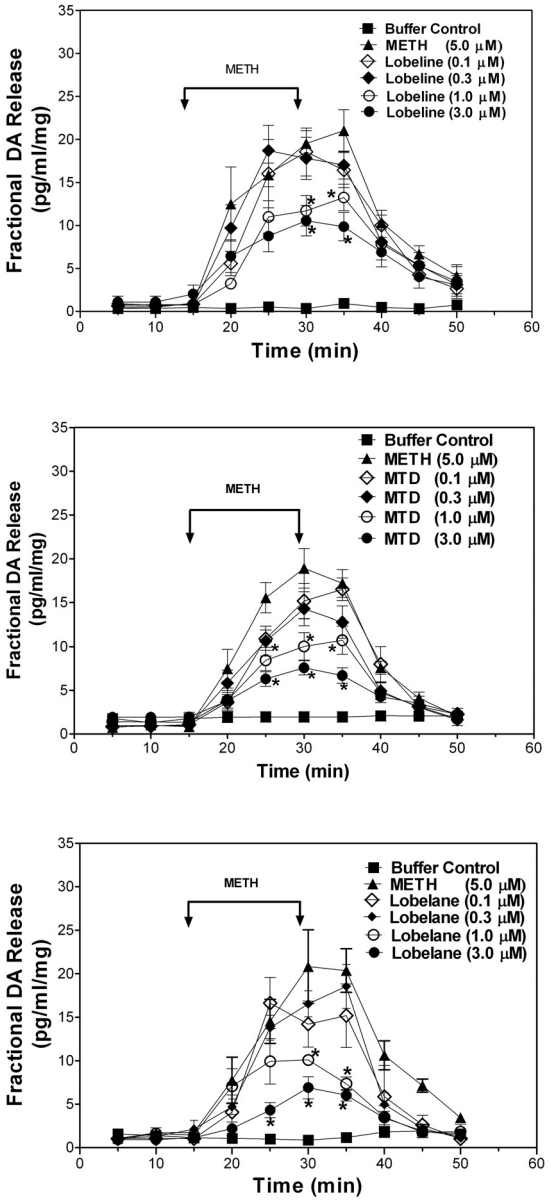

Fig. 8. Time course of lobeline, MTD and lobelane inhibition of methamphetamine-evoked fractional DA release from rat striatal slices. Top illustrates the time course of lobeline to inhibit methamphetamine-evoked fractional DA release. Middle illustrates the time course for MTD inhibition of methamphetamine-evoked fractional DA release. Bottom illustrates the time course for lobelane inhibition of methamphetamine-evoked fractional DA release. Data are expressed as pg/ml/mg (mean ± S.E.M) (*, $p < 0.05$ different from methamphetamine control; $n = 5$, 5, and 4 rats for lobeline, MTD, and lobelane, respectively).

The IC_{50} value for lobelane was 0.65 μM, and the I_{max} value was 73%. The time course for lobelane to inhibit methamphetamine-evoked fractional DA release is shown in Fig. 8 (bottom), and a concentration × time interaction ($F_{36,125}$ = 4.93, $p < 0.01$) was found. Lobelane at 1.0 μM significantly decreased methamphetamine-evoked fractional DA release from 30 to 35 min, and at 3.0 μM, lobelane decreased methamphetamine-evoked fractional DA release from 25 to 35 min.

(−)-*trans*-Lobelane, (+)-*trans*-Lobelane (−)-TTD, and (+)-TTD Inhibition of Methamphetamine-Evoked DA Overflow and the Time Course of Inhibition. Supplemental Fig. 1 (top) illustrates the inhibition of methamphetamine-evoked DA overflow by (−)-*trans*-lobelane and (+)-*trans*-lobelane. (−)-*trans*-Lobelane did not inhibit methamphetamine-evoked DA overflow. With respect to inhibition of methamphetamine-evoked fractional DA release, neither the main effect of concentration nor the concentration × time interaction were significant. Analysis of the inhibition of methamphetamine-evoked DA overflow by (+)-*trans*-lobelane showed a concentration effect ($F_{5,25}$ = 15.39, $p < 0.001$). Subsequent post hoc analysis revealed that the lowest concentration of (+)-*trans*-lobelane to inhibit methamphetamine-evoked DA overflow was 3 μM. The IC_{50} value for (+)-*trans*-lobelane was >3.0 μM, whereas the I_{max} value was 34%. The I_{max} value for lobelane was greater ($p < 0.05$) than that for (+)-*trans*-lobelane. A concentration × time interaction ($F_{36,225}$ = 1.84, $p < 0.01$) was found for (+)-*trans*-lobelane inhibition of methamphetamine-evoked DA release (data not shown). For (+)-*trans*-lobelane, 0.3 to 3.0 μM decreased ($p < 0.05$) methamphetamine-evoked fractional DA release only at 35 min.

Supplemental Fig. 1 also illustrates the inhibitory effect of the enantiomers of TTD on methamphetamine-evoked DA overflow. Concentration effects for (−)-TTD ($F_{5,27}$ = 20.518, $p < 0.001$) and (+)-TTD ($F_{5,18}$ = 20.48, $p < 0.001$) were found. The lowest concentration to inhibit ($p < 0.05$) methamphetamine-evoked DA overflow for (−)-TTD was 0.1 μM; the IC_{50} value was >3.0 μM, and the I_{max} value was 42%. The I_{max} value for MTD was greater ($p < 0.05$) than that for (−)-TTD. The lowest concentration of (+)-TTD to inhibit methamphetamine was 1 μM. The IC_{50} value was 0.22 μM, and the I_{max} value was 50%.

The time course of (−)-TTD- and (+)-TTD-induced inhibition of methamphetamine-evoked fractional DA release is illustrated in Supplemental Fig. 2. Inhibition of methamphetamine-evoked fractional DA release by (−)-TTD and (+)-TTD revealed concentration × time interactions ($F_{36,250}$ = 3.20, $p < 0.01$; $F_{36,170}$ = 4.15, $p < 0.01$, respectively). (−)-TTD (1.0–3.0 μM) decreased ($p < 0.05$) methamphetamine-evoked fractional DA release only at 30 min, whereas the inhibitory effect of (+)-TTD was more prolonged. At 3.0 μM, (+)-TTD decreased methamphetamine-evoked fractional DA release from 30 to 45 min. At 0.3 and 1.0 μM, (+)-TTD decreased fractional DA release from 35 to 45 min.

***nor*-MTD, (±)-*nor*-TTD, and *nor*-Lobelane Inhibition of Methamphetamine-Evoked DA Overflow.** The inhibitory effect of *nor*-MTD, (±)-*nor*-TTD, and *nor*-lobelane on methamphetamine-evoked DA overflow is illustrated in Supplemental Fig. 3. A concentration effect for *nor*-MTD ($F_{5,19}$ = 49.62, $p < 0.001$), (±)-*nor*-TTD ($F_{5,18}$ = 20.48, $p < 0.001$), and *nor*-lobelane ($F_{5,27}$ = 20.518, $p < 0.001$) was found. The lowest concentration to inhibit methamphetamine-evoked DA overflow was 0.3 μM, 0.1 μM, and 1 μM for *nor*-MTD, *nor*-lobelane, and (±)-*nor* -TTD, respectively. The IC_{50} value for *nor*-MTD was 0.40 μM, and the I_{max} value was 64%. Although IC_{50} values were greater than 3 μM for *nor*-lobelane and (±)-*nor*-TTD, I_{max} values of 47% and 34%, respectively, were obtained for the highest concentration of these analogs.

The time course for inhibition of methamphetamine-evoked fractional DA release by the *nor*-analogs is illustrated in Supplemental Fig. 4. A concentration × time interaction ($F_{36,195}$ = 3.66, $p < 0.01$) was found for *nor*-MTD, and the highest concentration tested (3.0 μM) decreased ($p < 0.05$) methamphetamine-evoked fractional DA release from 30 to 35 min. (±)-*nor*-TTD inhibition of methamphetamine displayed a concentration × time interaction ($F_{36,125}$ = 3.39, $p < 0.01$). (±)-*nor*-TTD at 1.0 μM decreased ($p < 0.05$) methamphetamine-evoked fractional DA release at 30 min, and at 3.0 μM from 30 to 35 min. A concentration × time interaction ($F_{36,215}$ = 3.30, $p < 0.01$) was also found for *nor*-lobelane, and 3.0 μM decreased ($p < 0.05$) methamphetamine-evoked fractional DA release at 35 min.

Lobelane and (+)-*trans*-Lobelane Increase DOPAC Overflow in the Presence of Methamphetamine. A concentration effect was found on DOPAC overflow for only lobelane and (+)-*trans*-lobelane ($F_{5,19}$ = 49.62, $p < 0.001$ and $F_{5,22}$ = 4.49, p = 0.005, respectively; data not shown). Lobelane (0.1–3.0 μM) and (+)-*trans*-lobelane (0.3 and 3.0 μM) increased ($p < 0.05$) DOPAC overflow compared with the methamphetamine control condition (data not shown).

Discussion

Lobeline has high affinity for VMAT2 and low affinity for DAT (Teng et al., 1997, 1998; Dwoskin and Crooks, 2002). Lobeline increased DOPAC overflow, but did not increase DA overflow (Teng et al., 1997; Miller at al., 2001), indicating alterations in presynaptic DA storage and lack of MAO inhibition (Dwoskin and Crooks, 2002). In the current study, low concentrations of lobeline inhibited methamphetamine-evoked DA release from rat striatal slices at concentrations that inhibited amphetamine-evoked DA release (Miller et al., 2001). The current study provides SAR for a larger group of defunctionalized lobeline analogs to identify selective, high-affinity inhibitors of VMAT2 that inhibit methamphetamine-evoked DA release.

In the synaptosomal [^{3}H]DA uptake assay assessing DAT function, lobelane markedly increased inhibitory potency, whereas MTD resulted in a further increase in potency compared to lobeline. An enantioselective effect was observed with the stereoisomers of MTD; (+)-TTD exhibited reduced potency at DAT relative to (−)-TTD, and both enantiomers exhibited decreased potency compared with MTD. This trend was not observed with the lobelane stereoisomers; (−)- and (+)-*trans*-lobelane were equipotent with each other and with lobelane. *N*-Demethylation of MTD and (−)-TTD resulted in decreased potency, whereas *N*-demethylation of lobelane increased potency. Collectively, these data demonstrate that defunctionalization of lobeline increases inhibitory potency at DAT, whereas effects of *N*-demethylation and C2,C6 stereochemistry on potency depend on the nature of the C_2 linker units.

With respect to analog interaction with VMAT2, MTD was

~5-fold less potent than lobeline at inhibiting [^{3}H]DTBZ binding, whereas (−)-TTD and (+)-TTD were equipotent with MTD inhibiting [^{3}H]DTBZ binding, indicating that piperidino C2,C6 stereochemistry is not a critical factor. Because both (−)-TTD and (+)-TTD lack affinity for α4β2* and α7* nAChRs (Zheng et al., 2005), these analogs are more selective for VMAT2 than either lobeline or MTD. *trans*-Isomers of lobelane were less potent than lobelane and lobeline inhibiting [^{3}H]DTBZ binding to VMAT2; (−)-*trans*-lobelane and (+)-*trans*-lobelane were equipotent and had 5-fold lower affinity at VMAT2 compared with lobelane, consistent with the premise that C2,C6 piperidino stereochemistry is not critical for VMAT2 interaction. Because (−)-*trans*-lobelane and (+)-*trans*-lobelane were inactive at α4β2* and α7* nAChRs (Zheng et al., 2005), these enantiomers are more selective for VMAT2 than lobeline, MTD, or lobelane. *nor*-MTD was 5-fold more potent than MTD at the [^{3}H]DTBZ binding site, and because *nor*-MTD did not interact with α4β2* and α7* nAChRs (Zheng et al., 2005), it had greater selectivity for VMAT2 than MTD. Likewise, *nor*-lobelane and lobelane were equipotent at VMAT2, but *nor*-lobelane was more selective for VMAT2. (±)-*nor*-TTD was equipotent with MTD at the VMAT2 binding site, but (±)-*nor*-TTD was more selective for VMAT2. Taken together, *N*-demethylation does not seem to alter affinity at the [^{3}H]DTBZ binding site, but improves VMAT2 selectivity.

A high degree of [^{3}H]DTBZ binding site affinity does not necessarily translate into functional inhibition of VMAT2. Therefore, the ability of these compounds to inhibit [^{3}H]DA uptake into synaptic vesicles was evaluated. Lobelane displayed a 10-fold increase in potency compared with lobeline inhibiting [^{3}H]DA uptake at VMAT2, and *nor*-lobelane was equipotent with lobelane. In contrast, (+)- and (−)-*trans*-lobelane exhibited markedly reduced inhibition of [^{3}H]DA uptake, indicating that whereas the *N*-methyl group is not critical, *cis*-stereochemistry of the defunctionalized, saturated compounds is a contributing structural characteristic for potent VMAT2 inhibition. MTD was equipotent with lobeline inhibiting [^{3}H]DA uptake, and was 10-fold less potent than lobelane. (+)-TTD, (−)-TTD, and (±)-*nor*-TTD were equipotent with MTD. However, nor-MTD had the lowest potency, whereas *nor*-lobelane and lobelane were equipotent in the VMAT2 functional assay. Thus, demethylation-induced changes in potency were most evident in the unsaturated MTD series of analogs.

In the methamphetamine-evoked DA overflow assay, MTD and lobelane had the best profile of inhibition. MTD inhibited methamphetamine-evoked DA overflow and was equipotent with lobeline; however, maximal inhibition was greater with MTD. (+)-TTD was equipotent with both MTD and lobeline inhibiting methamphetamine-evoked DA release; however, maximal inhibition produced by (+)-TTD was only 50%. Although maximal inhibition produced by the TTD enantiomers was not different, enantioselective effects on potency were observed. Lobelane was equipotent with lobeline, although lobelane exhibited greater maximal inhibition of methamphetamine-evoked DA release. (+)-*trans*-Lobelane was less potent than lobelane, and exhibited only 34% inhibition. (−)-*trans*-Lobelane did not inhibit methamphetamine. Thus, the combination of chemical defunctionalization and C2,C6-*cis*-stereochemistry affords analogs with a better profile for inhibition of methamphetamine effects.

nor-MTD was equipotent with MTD and exhibited similar maximal inhibition of methamphetamine-evoked DA release. Thus, removal of the methyl group in MTD did not alter its inhibitory profile. Because *nor*-MTD had no activity at α4β2* and α7* nAChRs, it is more selective for VMAT2 than MTD. *nor*-Lobelane had both a lower potency and lower maximal inhibition of the effect of methamphetamine compared with lobelane, which contrasts with its equipotent and complete inhibition of VMAT2 function. Thus, with respect to methamphetamine-evoked DA release, the *N*-methyl group improves the inhibitory profile in the saturated lobelane compounds, but has no impact in the unsaturated MTD series.

A comparison of results from the three assays reveals SAR inconsistencies and a different rank order of potencies. Inconsistencies in [^{3}H]DTBZ binding and vesicular [^{3}H]DA uptake to predict the ability of the analogs to inhibit methamphetamine were noted. For example, MTD was 5-fold less potent inhibiting [^{3}H]DTBZ binding than was lobeline, whereas MTD and lobeline had similar potencies inhibiting methamphetamine. Although both *trans*-lobelane enantiomers inhibited [^{3}H]DTBZ binding to VMAT2 equipotently, (+)-*trans*-lobelane showed only ~30% inhibition of methamphetamine-evoked DA release, whereas (−)-*trans*-lobelane exhibited no inhibition. In addition, (−)-*trans*-lobelane was a false positive, i.e., active in VMAT2 binding and uptake assays, but inactive in the methamphetamine-evoked DA release assay. Although both (+)-TTD and (−)-TTD inhibited [^{3}H]DTBZ binding equipotently, (−)-TTD had lower potency inhibiting methamphetamine. Potential interpretations of these results are that an additional site on VMAT2 or alternative vesicle protein sites are being targeted.

Lobelane exhibited the best overall profile, having high affinity at the VMAT2 binding site, high potency inhibiting VMAT2 function, low potency inhibiting DAT function, and potently and almost completely inhibiting methamphetamine-evoked DA release. Taking into account the greater selectivity for VMAT2 exhibited by lobelane compared with lobeline, lobelane has greater potential as a lead compound for the development of treatments for methamphetamine abuse. Lobelane-induced inhibition of VMAT2 function was 10-fold greater than lobeline, despite lobelane having only 2-fold greater affinity than lobeline for the [^{3}H]DTBZ binding site, suggesting that lobelane is acting at alternate sites on VMAT2 to inhibit function or that the mechanism of inhibition (i.e., competitive versus noncompetitive) is different between these two compounds. To elucidate the mechanism of action, saturation kinetic assays were conducted by use of the synaptic vesicle preparation. Results showed that both compounds inhibited vesicular [^{3}H]DA uptake competitively, supporting the contention that lobelane and lobeline act at different sites on VMAT2.

All analogs studied inhibited VMAT2 function. However, several potential underlying mechanisms by which these analogs inhibit methamphetamine are possible. Some of these analogs are probably interacting with DAT to inhibit the effects of methamphetamine to evoke DA release. Four analogs were equipotent in inhibiting DAT and VMAT2 function, including (−)-TTD, (+)-TTD, (+)-*trans*-lobelane, and (−)-*trans*-lobelane. Furthermore, MTD and *nor*-MTD inhibited DAT with 12- and 42-fold greater potency, respectively, than at VMAT2. Thus, the underlying mechanism for these analogs to inhibit methamphetamine-evoked DA release may be via inhibition of DAT function.

In contrast, lobeline and lobelane exhibited 67- and 35-fold greater potency, respectively, in inhibiting VMAT2 function than DAT function. Thus, there is a high likelihood that lobelane and lobeline are acting at VMAT2 to inhibit the effect of methamphetamine.

Another potential mechanism for analog-induced inhibition of methamphetamine-evoked DA release may be through facilitation of DA metabolism to DOPAC via redistribution of presynaptic DA from the vesicles to the cytosol. Once in the cytosol, DA would be available for metabolism to DOPAC by MAO. Although not considered "release" (i.e., exocytotic or transporter-mediated), extracellular DOPAC concentration is altered in response to neuronal activity and drugs, and essentially reflects increased dopaminergic neuron activity. These analogs produce no reduction in striatal DA content. Previous studies determining the mechanism of action of lobeline revealed increased [^{3}H]DA overflow from rat striatal slices in the presence of nomifensine and pargyline (DAT and MAO inhibitors, respectively), whereas in their absence, lobeline increased DOPAC overflow. In addition, lobeline inhibited both [^{3}H]DA uptake and elicited [^{3}H]DA release from synaptic vesicles. It is noteworthy that lobeline reduced methamphetamine-evoked DA overflow from striatal slices regardless of the presence or absence of pargyline (Dwoskin and Crooks, 2002). Together, these results indicate that lobeline redistributes presynaptic DA from synaptic vesicles to the cytosol, where it is metabolized to DOPAC by MAO, thus reducing the DA pool available for DAT-mediated reverse-transport after methamphetamine exposure. After interaction with VMAT2, altered DA redistribution and metabolism may contribute to the underlying mechanism responsible for lobelane-mediated inhibition of methamphetamine.

In summary, lobelane inhibits methamphetamine-evoked DA release and is more selective inhibiting VMAT2 than lobeline. Lobelane is 35-fold more potent as an inhibitor of VMAT2 function than DAT function, consistent with the interpretation that lobelane acts at VMAT2 to inhibit methamphetamine effects. Thus, lobelane is a promising lead for further development as a pharmacotherapeutic for methamphetamine abuse.

Acknowledgments

We thank Dr. Don Saucier for assistance with the statistical analyses and Dr. Michael Kilbourn for generously supplying [^{3}H]DTBZ.

References

Bowyer JF, Scallet AC, Holson RR, Lipe GW, Slikker W Jr, and Ali SF (1991) Interactions of MK-801 with glutamate-, glutamine- and methamphetamine-evoked release of [^{3}H]dopamine from striatal slices. *J Pharmacol Exp Ther* **257:** 262–270.

Briggs CA and McKenna DG (1998) Activation and inhibition of the human alpha7 nicotinic acetylcholine receptor by agonists. *Neuropharmacology* **37:**1095–1102.

Brown JM, Hanson GR, and Fleckenstein AE (2000) Methamphetamine rapidly decreases vesicular dopamine uptake. *J Neurochem* **74:**2221–2223.

Brown JM, Hanson GR, and Fleckenstein AE (2001) Regulation of the vesicular monoamine transporter-2: a novel mechanism for cocaine and other psychostimulants. *J Pharmacol Exp Ther* **296:**762–767.

Decker MW, Majchrzak MJ, and Arnerić SP (1993) Effects of lobeline, a nicotinic receptor agonist, on learning and memory. *Pharmacol Biochem Behav* **45:**571–576.

Di Chiara G and Imperato A (1988) Drugs abused by humans preferentially increase synaptic dopamine concentrations in the mesolimbic system of freely moving rats. *Proc Natl Acad Sci U S A* **85:**5274–5278.

Dwoskin LP and Crooks PA (2002) A novel mechanism of action and potential use for lobeline as a treatment for psychostimulant abuse. *Biochem Pharmacol* **63:**89–98.

Eyerman DJ and Yamamoto BK (2005) Lobeline attenuates methamphetamine-induced changes in vesicular monoamine transporter-2 immunoreactivity and monoamine depletions in the striatum. *J Pharmacol Exp Ther* **312:**160–169.

Flammia D, Dukat M, Damaj MI, Martin B, and Glennon RA (1999) Lobeline: structure-affinity investigation of nicotinic acetylcholinergic receptor binding. *J Med Chem* **42:**3726–3731.

Fleckenstein AE, Volz TJ, Riddle EL, Gibb JW, and Hanson GR (2007) New insights into the mechanism of action of amphetamines. *Annu Rev Pharmacol Toxicol* **47:**681–698.

Gold LH, Geyer MA, and Koob GF (1989) Neurochemical mechanisms involved in behavioral effects of amphetamines and related designer drugs. *NIDA Res Monogr* **94:**101–126.

Harrod SB, Dwoskin LP, Crooks PA, Klebaur JE, and Bardo MT (2001) Lobeline attenuates *d*-methamphetamine self-administration in rats. *J Pharmacol Exp Ther* **298:**172–179.

Harrod SB, Dwoskin LP, Green TA, Gehrke BJ, and Bardo MT (2003) Lobeline does not serve as a reinforcer in rats. *Psychopharmacology (Berl)* **165:**397–404.

Hart CL, Ward AS, Haney M, Foltin RW, and Fischman MW (2001) Methamphetamine self-administration by humans. *Psychopharmacology* **157:**75–81.

Institute of Laboratory Animal Resources (1996) *Guide for the Care and Use of Laboratory Animals,* 7th ed. Institute of Laboratory Animal Resources, Commission on Life Sciences, National Research Council, Washington, DC.

Liang NY and Rutledge CO (1982) Evidence for carrier-mediated efflux of dopamine from corpus striatum. *Biochem Pharmacol* **31:**2479–2484.

Lim DY, Kim YS, and Miwa S (2004) Influence of lobeline on catecholamine release from the isolated perfused rat adrenal gland. *Auton Neurosci* **110:**27–35.

Mantle TJ, Tipton KF, and Garrett NJ (1976) Inhibition of monoamine oxidase by amphetamine and related compounds. *Biochem Pharmacol* **25:**2073–2077.

Miller DK, Crooks PA, and Dwoskin LP (2000) Lobeline inhibits nicotine-evoked [^{3}H]dopamine overflow from rat striatal slices and nicotine-evoked $^{86}Rb^+$ efflux from thalamic synaptosomes. *Neuropharmacology* **39:**2654–2662.

Miller DK, Crooks PA, Teng L, Witkin JM, Munzar P, Goldberg SR, Acri JB, and Dwoskin LP (2001) Lobeline inhibits the neurochemical and behavioral effects of amphetamine. *J Pharmacol Exp Ther* **296:**1023–1034.

Miller DK, Crooks PA, Zheng G, Grinevich VP, Norrholm SD, and Dwoskin LP (2004) Lobeline analogs with enhanced affinity and selectivity for plasmalemma and vesicular monoamine transporters. *J Pharmacol Exp Ther* **310:**1035–1045.

Patel J, Mooslehner KA, Chan PM, Emson PC, and Stamford JA (2003) Presynaptic control of striatal dopamine neurotransmission in adult vesicular monoamine transporter 2 (VMAT2) mutant mice. *J Neurochem* **85:**898–910.

Pifl C, Drobny H, Reither H, Hornykiewicz O, and Singer EA (1995) Mechanism of the dopamine-releasing actions of amphetamine and cocaine: plasmalemmal dopamine transporter versus vesicular monoamine transporter. *Mol Pharmacol* **47:** 368–373.

Substance Abuse and Mental Health Services Administration (SAMHSA), Office of Applied Studies. *The DASIS Report—Primary Methamphetamine/Amphetamine Admissions to Substance Abuse Treatment: 2005*, 2008 Feb 7, SAMHSA, Rockville, MD. [Cited 2008 May 8] Available from: http://www.oas.samhsa.gov/2k8/methamphetamineTx/meth.htm.

Sulzer D, Chen TK, Lau YY, Kristensen H, Rayport S, and Ewing A (1995) Amphetamine redistributes dopamine from synaptic vesicles to the cytosol and promotes reverse transport. *J Neurosci* **15:**4102–4108.

Sulzer D and Rayport S (1990) Amphetamine and other psychostimulants reduce pH gradients in midbrain dopaminergic neurons and chromaffin granules: a mechanism of action. *Neuron* **5:**797–808.

Takahashi N, Miner LL, Sora I, Ujike H, Revay RS, Kostic V, Jackson-Lewis V, Przedborski S, and Uhl GR (1997) VMAT2 knockout mice: heterozygotes display reduced amphetamine-conditioned reward, enhanced amphetamine locomotion, and enhanced MPTP toxicity. *Proc Natl Acad Sci U S A* **94:**9938–9943.

Teng L, Crooks PA, and Dwoskin LP (1998) Lobeline displaces [^{3}H]dihydrotetrabenazine binding and releases [^{3}H]dopamine from rat striatal synaptic vesicles: comparison with d-amphetamine. *J Neurochem* **71:**258–265.

Teng L, Crooks PA, Sonsalla PK, and Dwoskin LP (1997) Lobeline and nicotine evoke [^{3}H]overflow from rat striatal slices preloaded with [^{3}H]dopamine: differential inhibition of synaptosomal and vesicular [^{3}H]dopamine uptake. *J Pharmacol Exp Ther* **280:**1432–1444.

Terry AV Jr, Williamson R, Gattu M, Beach JW, McCurdy CR, Sparks JA, and Pauly JR (1998) Lobeline and structurally simplified analogs exhibit differential agonist activity and sensitivity to antagonist blockade when compared to nicotine. *Neuropharmacology* **37:**93–102.

Toth PT and Vizi ES (1998) Lobeline inhibits Ca^{2+} current in cultured neurons from rat sympathetic ganglia. *Eur J Pharmacol* **363:**75–80.

Wilhelm CJ, Johnson RA, Eshleman AJ, and Janowsky A (2008) Lobeline effects on tonic and methamphetamine-induced dopamine release. *Biochem Pharmacol* **75:** 1411–1415.

Wise RA (2002) Brain reward circuitry: insights from unsensed incentives. *Neuron* **36:**229–240.

Xu DD, Mo ZX, Yung KK, Yang Y, and Leung AW (2008) Individual and combined effects of methamphetamine and ketamine on conditioned place preference and NR1 receptor phosphorylation in rats. *Neurosignals* **15:**322–331.

Yokel RA and Pickens R (1973) Self-administration of optical isomers of amphetamine and methylamphetamine by rats. *J Pharmacol Exp Ther* **187:**27–33.

Zheng G, Dwoskin LP, Deaciuc AG, Norrholm SD, and Crooks PA (2005) Defunctionalized lobeline analogues: structure-activity of novel ligands for the vesicular monoamine transporter. *J Med Chem* **48:**5551–5560.

Address correspondence to: Dr. Linda Dwoskin, College of Pharmacy, University of Kentucky, Lexington, KY 40536-0082. E-mail: ldwoskin@email.uky.edu